Spatial relationships between soil moisture patterns and topographic variables at multiple scales in a humid temperate forested catchment

Geneviève A. Ali,[1] André G. Roy,[1] and Pierre Legendre[2]

Received 23 October 2009; revised 14 May 2010; accepted 21 May 2010; published 15 October 2010.

[1] New tools are needed in hydrology to improve our understanding of process heterogeneity and its relationship to catchment topography. We tested the distance-based Moran's eigenvector maps (DBMEM) method, which models patterns using a combination of positively and negatively autocorrelated structures, searching for soil moisture characteristic scales in a temperate humid forested system. We focused on three questions: (1) What are the characteristic spatial scales of shallow soil moisture? (2) Is there a strong relationship between soil moisture patterns and topographic variables at these scales? and (3) Which hydro-meteorological variables influence soil moisture scales and topographic controls in a significant way? Data consisted of 16 surveys of soil moisture at depths of 5, 15, 30, and 45 cm in the 5.1 ha Hermine catchment (Laurentians, Canada). The global DBMEM model explained 21 to 96% (adjusted R square) of the spatial variations in soil moisture apportioned into decreasing fractions over six spatially nested, additive submodels: very large (0.85–1.4 ha), large (0.54–0.85 ha), meso (0.50–0.54 ha), fine positive (0.22–0.50 ha), fine negative (0.10–0.22 ha), and very fine (0.02–0.10 ha). The effects of catchment topography (e.g., slope and contributing area) on soil moisture were significant at large and very large scales. Moisture patterns at these scales were dependent on previous storm properties and were good predictors of catchment response. The DBMEM approach provided insightful quantitative evidence regarding the temporal dependency of the relationships between dynamic soil moisture content and static topographic variables across scales.

Citation: Ali, G. A., A. G. Roy, and P. Legendre (2010), Spatial relationships between soil moisture patterns and topographic variables at multiple scales in a humid temperate forested catchment, *Water Resour. Res.*, *46*, W10526, doi:10.1029/2009WR008804.

1. Introduction

[2] Soil moisture is a critical hydrological state variable since its spatiotemporal variation indicates the presence of "active" or "contributing" areas and periods [*Ambroise*, 2004]. It is often used to determine if a catchment is characterized as being in a dry or wet state. Throughout this paper, the phrases "dry state" and "wet state" do not refer to evaporation dynamics but rather to the spatial organization of soil moisture. The dry state is when moisture patterns are disorganized because of the influence of local catchment attributes (e.g., soil and vegetation characteristics and terrain slope) and the predominance of vertical soil water fluxes [*Grayson et al.*, 1997]. The wet state occurs when moisture patterns are highly organized/connected due to the influence of nonlocal factors (e.g., upslope contributing area) and the predominance of lateral soil water fluxes [*Grayson et al.*, 1997]. These states stress the effects of various topographic controls on soil moisture [*Western et al.*, 2002]. The reference to local and nonlocal control factors implies that the issue of spatial scale must be carefully considered while investigating hydrological processes. Here, "scale" refers to the spatial size of a phenomenon while "scaling" refers to the transfer of information between scales. Scale and scaling issues are critical in complex hydrological systems, since catchment dynamics are the result of intertwined processes that are hierarchically structured. Processes occurring at a broad scale may be the result of other processes interacting at finer scales, yet the emergent behavior is not the exact sum of the parts [*Sivapalan and Young*, 2005]. It is therefore crucial to identify the controlling variables and to assess if their relative influence on emergent soil moisture patterns depends on the chosen scale of observation.

[3] One challenge concerns the choice of the most appropriate mathematical approach to discriminate and better understand scale-dependent hydrological mechanisms. *Schulz et al.* [2006, p. 1] called for the use of techniques aimed at providing a new mathematical description and quantification of structure and pattern building processes at different scales. To achieve such a description and quantification, one can either work with single-scale methods repeatedly at different scales or use alternative methods that contain

[1]Chaire de Recherche du Canada en Dynamique Fluviale, Département de Géographie, Université de Montréal, Montréal, Quebec, Canada.

[2]Département de Sciences Biologiques, Université de Montréal, Montréal, Quebec, Canada.

0043-1397/10/2009WR008804

multiple-scale components in their mathematical formulation [*Wu et al.*, 2000]. That is notably the case for semivariance analysis [e.g., *Western et al.*, 1999; *Skøien et al.*, 2003; *Western et al.*, 2004], wavelet analysis [e.g., *Redding et al.*, 2003], spectral analysis [e.g., *Cassel et al.*, 2000], and fractal analysis [e.g., *Kumar*, 1999; *Green and Erskine*, 2004]. *Klemeš* [1983, p. 1] stated: "We cannot impose scale but have to search for those which exist and try to understand their relationships and patterns." It implies that natural variables have their own distinctive range of spatial scales that characterize their behavior. Characteristic scales are the successive levels in a hierarchy that are associated with scale breaks and are thus easily differentiable [*Wu and Li*, 2006]. These scales can be derived from a semivariogram analysis of spatial patterns [*Skøien et al.*, 2003] or from Fourier analyses and harmonic regressions [*Blöschl*, 2001]. Quantification of spatial structure can also be obtained through trend surface analysis which models spatial gradients with polynomial regressions [*Legendre and Legendre*, 1998]. A major drawback of these methods is that they only allow for the very broadscale spatial variation to be modeled while finer spatial features remain undetected. This issue may, however, be resolved if examined in the framework of Moran's eigenvector maps (MEMs).

[4] MEMs are a recent family of spatial analysis techniques gaining popularity in ecology and fluid dynamics [*Borcard et al.*, 2004; *Brind'Amour et al.*, 2005; *Dray et al.*, 2006; *Griffith and Peres-Neto*, 2006; *Bellier et al.*, 2007; *Lacey et al.*, 2007; *Roy et al.*, 2009] but still unused in hydrology. They include spatial-filtering methods (e.g., distance-based Moran's eigenvector maps (DBMEMs) and principal coordinates of neighbor matrices (PCNMs)) which rely on the diagonalization of a spatial connectivity matrix. The eigenvectors computed from the spatial connectivity matrix represent the decomposition of the Moran coefficient of spatial autocorrelation into all mutually orthogonal and linearly uncorrelated map patterns [*Griffith and Peres-Neto*, 2006]. There is precedence in using the Moran coefficient in catchment hydrology. In a study of 10 catchments with different terrain characteristics and climatic regimes, *Cai and Wang* [2006] notably found a critical extent area of 1 km^2 over which the spatial autocorrelation of the topographic index becomes weak and static. These results refer to the representative elementary area concept [*Woods et al.*, 1995] and show the existence of threshold scales. *Cai and Wang* [2006] also detected a range of digital elevation model resolutions within which spatial autocorrelation was invariant. These findings underline the effect of sampling designs and data accuracy on our ability to capture scale-dependent processes. At first, the PCNM method was developed to dissect one-dimensional or two-dimensional spatial patterns across the whole range of scales perceptible within a given data set [*Borcard and Legendre*, 2002]. It achieves a spectral decomposition of the sampling space to describe the dominant spatial scales to which a given variable can potentially respond. The PCNM method therefore allows one to identify the fraction of the total variation in a dependent variable that is spatially structured [*Lacey et al.*, 2007]. It was later found that PCNMs are a particular case of DBMEM in the MEM framework (PCNM $\subset$ dbMEM $\subset$ MEM), the difference between DBMEMs and PCNMs residing in their approximation of the Moran coefficient of spatial autocorrelation [*Dray et al.*, 2006]. Regardless of whether DBMEMs or PCNMs are computed, the eigenvectors extracted from the spatial connectivity matrix are similar; they can be used as explanatory variables in multiple regression analysis to study the spatial structure of a single variable or in multivariate constrained ordination methods (e.g., canonical redundancy analysis) to study multiple variables at once. The MEM framework therefore enables us to link dominant spatial scales of the response variable(s) (e.g., soil moisture) to the spatial patterns of environmental variables (e.g., topography). It is not aimed at depicting pairwise relationships (e.g., connectivity) between point locations but rather at modeling the correlation structure present at each scale and linking this structure to the spatial heterogeneity of environmental factors. Identifying characteristic scales through the application of the DBMEM procedure would substantially enhance our understanding of hydrological processes and their scaling properties.

[5] Here, we introduce the MEM framework as a new, promising ensemble of spatial statistical techniques for hydrology. For illustration purposes, we applied the DBMEM method to investigate the spatial scale dependency of soil moisture content in a headwater temperate humid forested catchment. There are few studies, if any, that have used multivariate statistics to describe the spatial dependency of soil moisture and to quantify the effects of topographic controls on this variable. This study addresses three questions regarding soil moisture content and scale:

[6] 1. What are the characteristic spatial scales of shallow soil moisture?

[7] 2. Is there a strong relationship between soil moisture patterns and topographic variables at these scales?

[8] 3. Which hydrometeorological variables influence soil moisture scales and topographic controls in a significant way?

[9] This paper demonstrates that the DBMEM procedure provides some insightful, quantitative answers to these questions for a specific catchment.

2. Field Measurements

2.1. Study Site

[10] This study was done within a 5.1 ha headwater temperate humid forested catchment, the Hermine, located in the Lower Laurentians natural province about 80 km north of Montréal, Québec, Canada (45°59'N, 74°01'W, elevation c. 400 m) (Figure 1a). An intermittent first-order stream flows east to west in the valley of the catchment, which has an elongated open booklike shape. Relief is moderate, with a maximum elevation change of 31 m from the lowest valley location to the highest point in the catchment. The forest floor has a complex microtopography, partially due to fallen tree trunks and boulders at the soil surface. The total annual precipitation to the watershed averages 1150 mm (± 136 mm) over the last 30 years, of which about 30% falls as snow [*Biron et al.*, 1999].

[11] Soils are 1 to 2 m deep bouldery podzols developed over a glacial till. The occurrence of rapid lateral shallow subsurface flow and the formation of humid source areas are highly frequent at the Hermine, given a confining soil layer at a depth of 50 to 75 cm that restricts root penetration and slows water infiltration. Data from wells installed at nine riparian, midslope and upslope 300 m^2 sampling plots in the catchment and monitored over the last 12 years confirm that

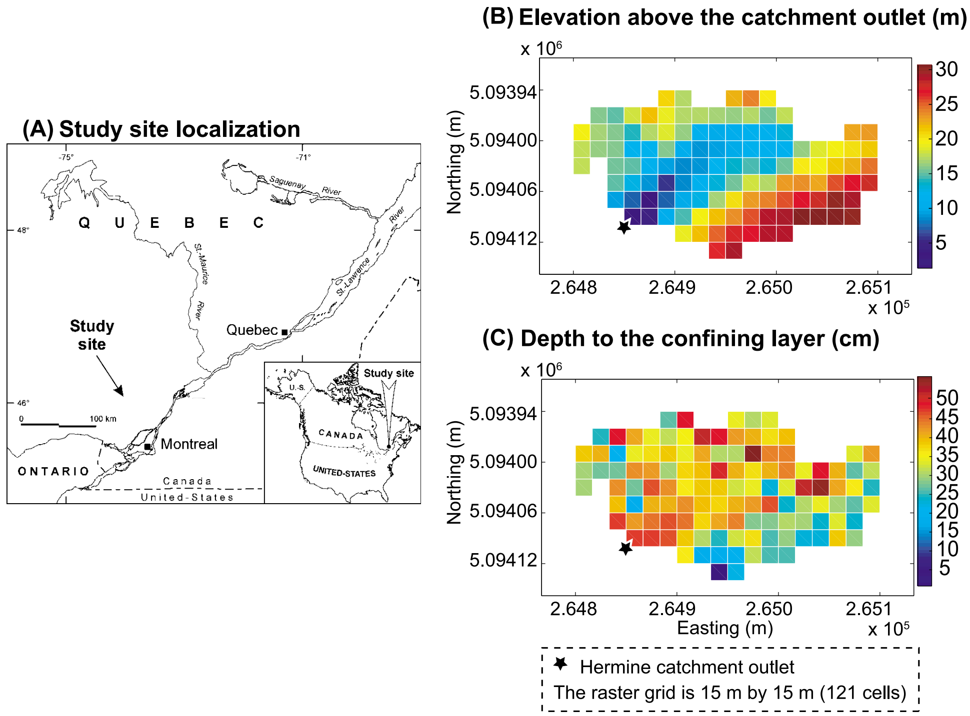

Figure 1. (a) Location of the Hermine catchment, (b) surface digital elevation model, and (c) depth to the confining soil layer.

the perched water table fluctuates between 1 and 108 cm below the soil surface (mean value: 68 cm). The occurrence of perched water tables is, however, sporadic during summer seasons, and surface runoff hardly ever happens due to interception of the forest canopy, uptake from the trees, and high potential evapotranspiration. Between October and April, transpiration is minimal, so that changes in soil moisture and the water table during that period are mostly governed by snow-related processes and downslope drainage.

2.2. Soil Moisture Monitoring

[12] Volumetric moisture content in the top 5, 15, 30, and 45 cm of the soil profile was measured in the Hermine catchment using a 15 m by 15 m sampling grid, for a total of 121 cells. Measurements were taken using a portable 30 in. long rod equipped with a capacitance-based probe (AQUATERR Instruments and Automation). Sixteen surveys were collected between August 2007 and July 2008 to capture patterns associated with various antecedent conditions and hydrologic responses at the catchment outlet. Figure 2 shows examples of soil moisture patterns. Table 1 provides a list of hydrometeorological variables that were used in this study to illustrate antecedent conditions and hydrologic responses, while Table 2 contains the specific values of selected hydrometeorological characteristics for the 16 soil moisture surveys. These variables were meant to help us assess the hydrometeorological dependence of the soil moisture patterns and their scaling properties.

2.3. Topographic Variables

[13] A surface digital elevation model (DEM) of the Hermine catchment (horizontal resolution: 1 m) was obtained by interpolating 640 elevation points collected in the field [*Drouin*, 1999] with a smooth simple natural neighbor algorithm (see *Sibson* [1981] for details on the interpolation method). Bilinear resampling was used to convert the interpolated data into a 15 m resolution surface DEM (Figure 1b) so that soil moisture data and elevation data were at the same scale of observation. The depth to the confining layer was measured on 257 points using a small hand auger that was forced vertically through the soil profile to refusal. For each sampling location, three auger-to-refusal measurements were made in a 1 m radius and checked for consistency to discard data associated with individual rocks rather than the impermeable layer. The data were interpolated at a 15 m resolution, thus giving a map (Figure 1c) having the same resolution as the surface DEM and the soil moisture surveys results.

[14] For each sampling square, elevation above the catchment outlet and depth to the confining layer were extracted. From the surface DEM, the terrain slope, the upslope contributing area, and the topographic index [*Beven and Kirkby*, 1979] were also computed for each sampling square using the D8 [*O'Callaghan and Mark*, 1984] and the D∞ [*Tarboton*, 1997] algorithms. These topographic variables were then put in two groups to illustrate possible local and nonlocal controls on soil moisture patterns. Terrain slope and depth to the confining soil layer were considered as local influences (hereafter called "local" variables or controls), while the elevations above the catchment outlet, the upslope contributing area, and the topographic index were assumed to represent nonlocal influences (hereafter called "nonlocal" variables or controls). To account for potential nonlinear topographic controls on soil moisture, the quadratic and cubic functions of each topo-

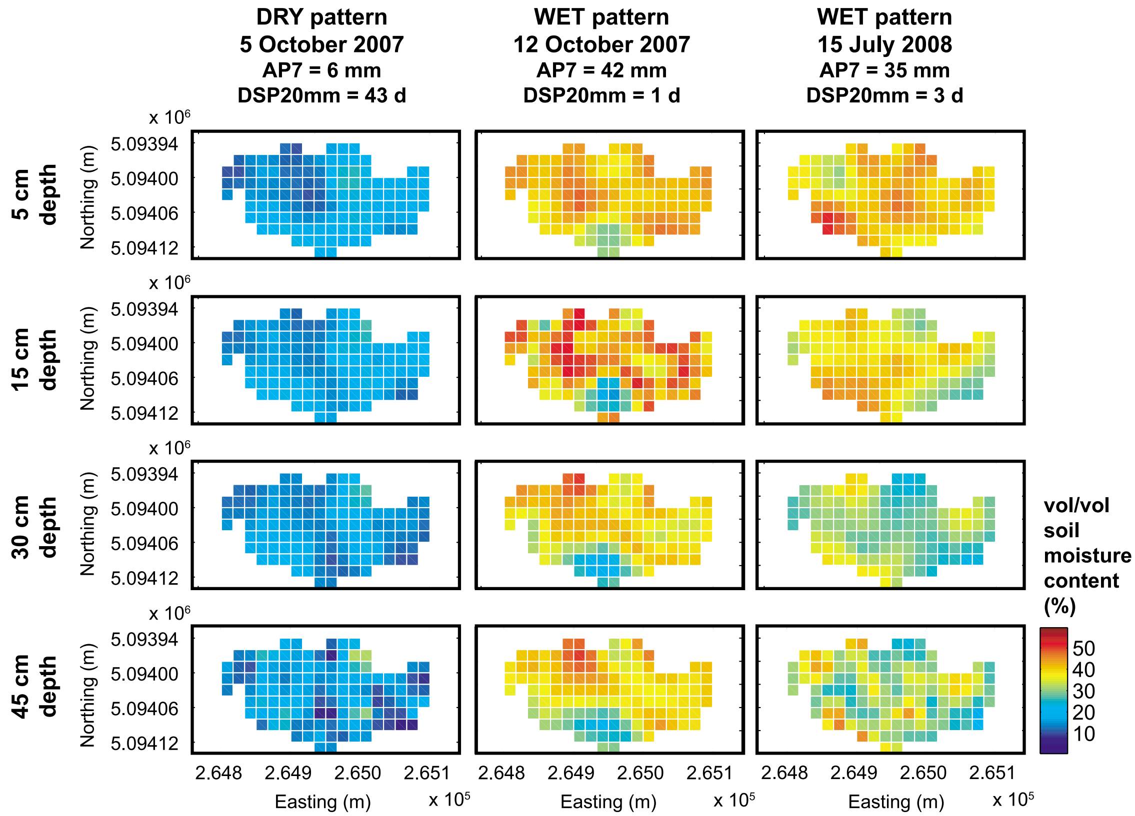

Figure 2. Sample soil moisture maps obtained after three contrasted surveys in the Hermine catchment.

graphic variable were also included in the local and nonlocal groups of variables. The local and nonlocal groups of variables were meant to be used as explanatory matrices in subsequent regression analyses.

3. Analytical Methods

[15] The MEM framework stands apart from traditional spatial analysis methods such as geostatistics. Geostatistical methods aim to explain how variance and covariance depend on the distance between observations. They model spatial structure by fitting a variogram function to an empirical variogram, assuming that the variable under study can be represented by a second-order stationary spatial process [*Bellier et al.*, 2007]. Geostatistics are therefore referred to as a model-based approach. Moran's eigenvector maps rather appear as a nonparametric method, as they do not presume any form of spatial structure. Specifically, the DBMEM method is a spatial filtering technique [*Blanchet et al.*, 2008] proceeding in two major stages: (1) the definition of a set of spatial proxy variables (this is done by means of a spatial connectivity matrix indicating the strength of the potential interaction between spatial units), and (2) the selection of the most important spatial proxy variables to explain the spatial structure of the variable under study. The definition of a spatial connectivity matrix only relies on the geographic coordinates of the sampling sites, hence the reference to a design-based approach. Regression or canonical analyses are later performed to associate the variable under study to a subset of spatial proxy variables. Specific analytical steps related to stages 1 and 2 of the DBMEM method are described in sections 3.1 and 3.2, respectively, and in Figure 3.

3.1. DBMEM Generation

[16] The steps involved in the generation of DBMEM are illustrated in Figure 3 and summarized below:

[17] 1. Starting from the x-y coordinates of the sampling grid locations, a Euclidean distance matrix D is calculated to store all possible distances d_{ij} between sampling locations i and j ($D = [d_{ij}]$).

[18] 2. A spatial connectivity function called W is constructed by truncating D at a threshold distance (or truncation distance) d_t as follows [*Borcard and Legendre*, 2002; *Dray et al.*, 2006; *Griffith and Peres-Neto*, 2006]:

$$W = (w_{ij}) = \begin{cases} 4 \times d_t & \text{if } d_{ij} > d_t \\ d_{ij} & \text{if } d_{ij} \leq d_t \end{cases} \tag{1}$$

Matrix W is therefore a truncated matrix in which not all sites are connected. Each nonnull weight w_{ij} indicates the possible connection between sites i and j, and the actual value of w_{ij} illustrates the strength of the potential interaction between the two spatial units i and j [*Dray et al.*, 2006]. The threshold distance d_t is estimated by computing a minimum spanning tree on D and it is either equal to or larger than the length of the longest link in the minimum spanning tree; that length represents the shortest distance required to maintain the graph of all locations connected [*Borcard et al.*, 2004; *Lacey et al.*, 2007].

Table 1. Hydrometeorological Variables Used as Surrogates for Antecedent Conditions and Hydrologic Responses in the Hermine Catchment

Variable	Description
Surrogates for Antecedent Conditions	
MSMC (%)	Catchment mean soil moisture content
PET (mm/d)	Potential evapotranspiration [*Hargreaves*, 1975] on day of survey
Rainfall (mm)	Rainfall on day of survey
AP2 (mm)	Cumulative precipitation from 2 days before survey; indicative of short-term antecedent conditions
AP5, AP7	Cumulative precipitation from 5 and 7 days before survey; indicative of medium-term antecedent conditions
AP12, AP14	Cumulative precipitation from 12 and 14 days before survey; indicative of long-term antecedent conditions
DSP (d)	Days since precipitation Number of days since last recording at rain gauge
DSP5mm (d)	Number of days since last rainfall intensity exceeding 5 mm/d
DSP10mm (d)	Number of days since last rainfall intensity exceeding 10 mm/d
DSP20mm (d)	Number of days since last rainfall intensity exceeding 20 mm/d
DSP30mm (d)	Number of days since last rainfall intensity exceeding 30 mm/d
PD_Discharge (mm/d)	Catchment discharge on day preceding survey
Surrogates for Hydrologic Response	
CD_Discharge (mm/d)	Catchment discharge on day of survey
DA1_Discharge (mm/d)	Catchment discharge on day following survey
DA2_Discharge (mm/d)	Catchment discharge in 2 days following survey
DA3_Discharge (mm/d)	Catchment discharge in 3 days following survey
DA4_Discharge (mm/d)	Catchment discharge in 4 days following survey
DA5_Discharge (mm/d)	Catchment discharge in 5 days following survey
DA6_Discharge (mm/d)	Catchment discharge in 6 days following survey
DA7_Discharge (mm/d)	Catchment discharge in 7 days following survey

[19] 3. Given that n is the number of sampling locations, I is an $n \times n$ identity matrix, $\mathbf{1}$ is an $n \times 1$ vector of ones, and t represents matrix transpose, the eigenvectors (DBMEM) of the centered connectivity matrix (equation (2)) are computed:

$$\Omega = (I - \mathbf{11}^t/n)W(I - \mathbf{11}^t/n) \quad (2)$$

Each eigenvector has a specific value for each sampling point, thus allowing the transition from the original location data to the eigenvector maps (see bubble maps in Figure 3). The black and white circles in the bubble maps illustrate possible autocorrelation patterns to which the variable under study (e.g., soil moisture) may or may not correspond. Matrix W is non-Euclidean, because not all connections among the sampling sites are considered after truncation. Thus, the DBMEM procedure yields both positive and negative eigenvalues. According to *Griffith and Peres-Neto* [2006], W is also a term appearing in the numerator of the Moran coefficient of spatial autocorrelation. Hence, eigenvectors obtained from Ω represent the decomposition of the Moran coefficient into mutually orthogonal and linearly uncorrelated map patterns. The Moran coefficient (MC) associated with each eigenvector v can be estimated as follows:

$$\mathrm{MC}(v) = \frac{n}{\mathbf{1}^t W \mathbf{1}} v^t W v \quad (3)$$

The values of the MC are in the range $[(n/\mathbf{1}^t\ \mathrm{W}\mathbf{1})\lambda_{\min},\ (n/\mathbf{1}^t\ \mathrm{W}\mathbf{1})\lambda_{\max}]$, given that $\lambda_{\min}$ and $\lambda_{\max}$ are the extreme eigenvalues of Ω [*Dray et al.*, 2006]. As a result, DBMEMs corresponding to small absolute eigenvalues represent fine scales and patchy spatial patterns in which spatial autocorrelation is low and spatial structures are difficult to discern. On the contrary, DBMEMs corresponding to large absolute eigenvalues represent large or coarse scales of variability and are very suitable to define spatial structures (see bubble maps in Figure 3). Also, DBMEMs paired with positive eigenvalues depict a positive spatial association, whereas DBMEMs paired with negative eigenvalues depict a negative spatial association [*Griffith and Peres-Neto*, 2006]. DBMEMs are able to model a wide range of spatial features

Table 2. Value of Selected Hydrometeorological Variables Associated With the 16 Soil Moisture Surveys in the Hermine Catchment[a]

Survey Date	MSMC (%)	AP7 (mm)	AP14 (mm)	PD_Discharge (mm/d)	CD_Discharge (mm/d)	DA1_Discharge (mm/d)
6 August 2007	33.8	4	36	0.0066	0.6619	0.2721
13 August 2007	23.3	44	48	0.0766	0.2224	0.0677
7 September 2007	27.0	8	44	0.0376	0.0486	0.0172
14 September 2007	29.0	14	22	0.0486	0.0667	0.4960
21 September 2007	27.7	18	32	0.0769	0.0649	0.0462
28 September 2007	27.9	4	22	0.0306	0.0980	0.1354
5 October 2007	17.3	6	10	0.0881	0.0881	0.0881
12 October 2007	39.6	42	48	0.2483	5.8726	3.0560
26 October 2007	23.1	43	67	1.0059	0.9087	4.3714
2 November 2007	21.5	33	76	1.3622	1.5208	1.4634
9 November 2007	21.1	17	50	2.0025	1.7077	1.4937
20 May 2008	34.4	39	54	0.9484	1.7975	1.0892
2 June 2008	30.0	29	61	0.8787	0.8288	0.8288
17 June 2008	32.2	29	37	0.5245	0.5241	0.4877
15 July 2008	31.5	43	59	0.5325	0.4193	0.3667
21 July 2008	35.2	35	75	0.9026	0.7835	1.4204

[a]See Table 1 for descriptions of hydrometeorological variables at the top of each column.

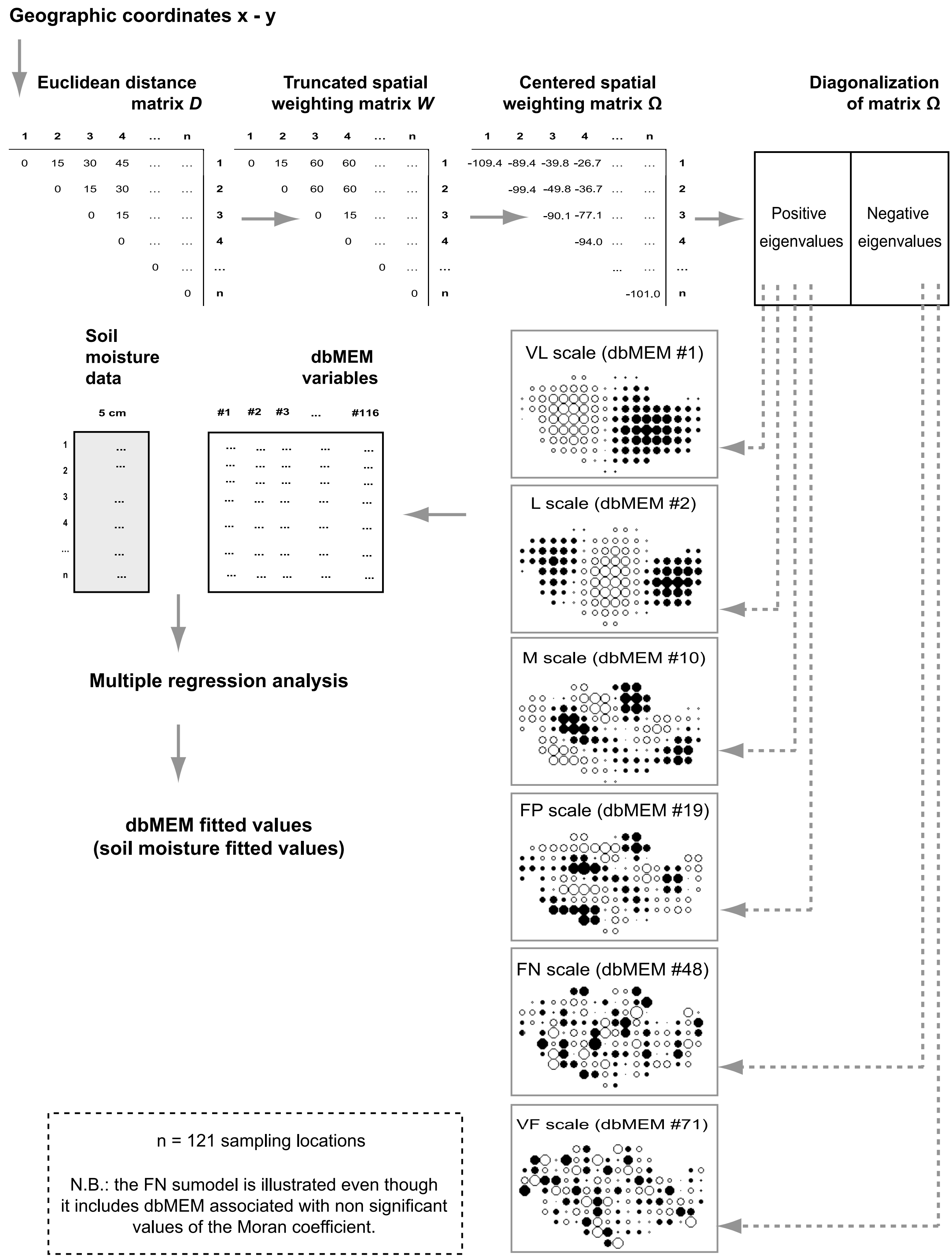

Figure 3. Methodology for developing distance-based Moran's eigenvector map (DBMEM) variables and obtaining soil moisture fitted values (DBMEM fitted values). B, broad; VL, very large; L, large; M, meso; FP, fine positive; FN, fine negative; VF, very fine.

from planes, saddles, and parabolas representing bumps or troughs to random autocorrelated variables [*Borcard and Legendre*, 2002; *Dray et al.*, 2006]. All obtained eigenvectors are orthogonal to one another (i.e., their scalar product is null), with the consequence that their explained variation is additive. They represent nested spatial scales. These DBMEMs (also called spatial eigenfunctions or spatial base functions) are spatial predictors/filters that can be used as explanatory variables in any classical statistical analysis.

[20] For regularly spaced points, DBMEMs are similar to a series of sine waves of decreasing periods [*Borcard and Legendre*, 2002]. However, the DBMEM method does not only apply to periodic spatial processes, as the flexible combination of sine waves can model nonlinear features of any shape [*Borcard et al.*, 2004]. DBMEM analysis does optimally when uniform sampling grids are used, but it still does well with points having irregularly spaced x and y coordinates [*Borcard and Legendre*, 2002; *Lacey et al.*, 2007]. The largest detectable scale corresponds to the DBMEM variable with the largest period, which is dictated by the distance between the furthest sampling locations [*Lacey et al.*, 2007]. The technique cannot detect scales smaller than the threshold distance d_t [*Borcard and Legendre*, 2002].

3.2. Characterization of Relevant Spatial Scales

[21] Spatial eigenfunctions obtained from DBMEM analysis form a global model which can explain a certain amount of the soil moisture patterns' spatial variation. This global model can be decomposed into individual DBMEM submodels or into nested submodels, each containing several eigenfunctions, to unravel the hierarchical levels at which processes may be the most important. The selection of the number of submodels and their associated scales is subjective and is generally decided upon consideration of the research objectives and the similarity between the periods of the significant eigenfunctions [*Lacey et al.*, 2007].

[22] Here, we chose to study each of the 64 soil moisture patterns (16 dates × 4 depths) individually rather than considering all four depths from each survey in a multivariate framework. In doing so, we investigated whether surface or subsurface patterns of hydrologic properties should be used to predict our catchment response. This choice is particularly crucial in humid temperate systems that are thought to be dominated by subsurface stormflow [*Weiler et al.*, 2005]. Hence, it is important to study the scales at which bedrock-induced and confining layer-induced saturated areas occur at different levels in the soil column [*Tromp-Van meerveld and McDonnell*, 2006]. Besides, nonparametric Kruskal-Wallis tests showed that our soil moisture patterns were significantly different ($p < 0.05$) among both survey dates and studied depths, thus calling for an individual analysis. A regression analysis was therefore run with each moisture pattern as the response variable and each spatial DBMEM submodel, in turn, as the explanatory variable. We took advantage of the orthogonal property of the spatial eigenfunctions, which implies that the variations explained by the various DBMEM submodels are additive. The contribution of each DBMEM submodel to the explanation of each moisture pattern was quantified using the coefficient of determination or R squared (R^2). We examined a global DBMEM model that was decomposed into six distinct and additive spatial submodels: very large (VL), large (L), meso (M), fine positive (FP), fine negative (FN) and very fine (VF) as in:

$$R^2_{\text{global}} = R^2_{\text{VL}} + R^2_{\text{L}} + R^2_{\text{M}} + R^2_{\text{FP}} + R^2_{\text{FN}} + R^2_{\text{VF}} \tag{4}$$

The higher the value of R^2, the higher the explained spatial variation in soil moisture at a particular scale. While the VL, L, M, and FP scales represent positive spatial autocorrelation, the FN and VF scales represent the negative spatial association. The adjusted R square R^2_α was used in addition to the "unadjusted" one. Unlike R^2, R^2_α has the advantage of allowing the comparison of regression equations involving different numbers of objects and explanatory variables, and its value increases only if a new explanatory variable improves the model more than would be expected by chance. R^2_α can take negative values in the case of a low ratio of observations to regressors, thus suggesting the absence of a link between the variables that are being tested. Equation (4), however, does not hold when R^2_α is used [*Lacey et al.*, 2007]. The global spatial model (containing all DBMEMs) and each of the six submodels were tested for significance ($p < 0.05$) using 999 Monte Carlo unrestricted permutations. Multiple regressions yielded "fitted soil moisture values" (hereafter called "DBMEM fitted values") that were kept for further analysis.

3.3. Data Detrending

[23] *Borcard et al.* [2004] suggested checking the response data (e.g., soil moisture patterns) for linear trends before DBMEM analysis. Such trends indicate the presence of a spatial structure at a scale broader than the sampling extent. The use of undetrended and nonstationary data is not problematical for DBMEM analysis, except that it compromises the modeling of fine-scale spatial features. In such cases, half of the available DBMEM variables would be used only to model the broadscale, trend while finer-scale features could go undetected. Each soil moisture pattern was therefore detrended by removing its spatial linear gradient. This was achieved by multiple regressions involving only the x and y coordinates as explanatory variables and the soil moisture data for each survey, in turn, as a response variable. The linear gradient removed from each pattern was then considered as a seventh spatial predictor, the broad (B) scale, in addition to the DBMEMs associated with the VL, L, M, FP, FN and VF scales. As the B scale is not a DBMEM-derived model, however, it does not share the additive property that the VL, L, M, FP, FN, and VF scales have. Multiple regressions yielded fitted soil moisture values (hereafter called "trend fitted values") that are used for further analysis.

3.4. Scale-Dependent Relationships Between Moisture Patterns and Topographic Variables

[24] Lastly, we linked the spatial structure in soil moisture patterns to the influence of topographic variables. This was achieved by using the trend fitted values or the DBMEM fitted values of each submodel as a response variable and the topographic (explanatory) variables in the variation partitioning analyses. In this common method, one partitions the variation of a response variable (or data table) among two or more sets of explanatory variables using a series of regressions (or canonical analyses). The adjusted R squares of

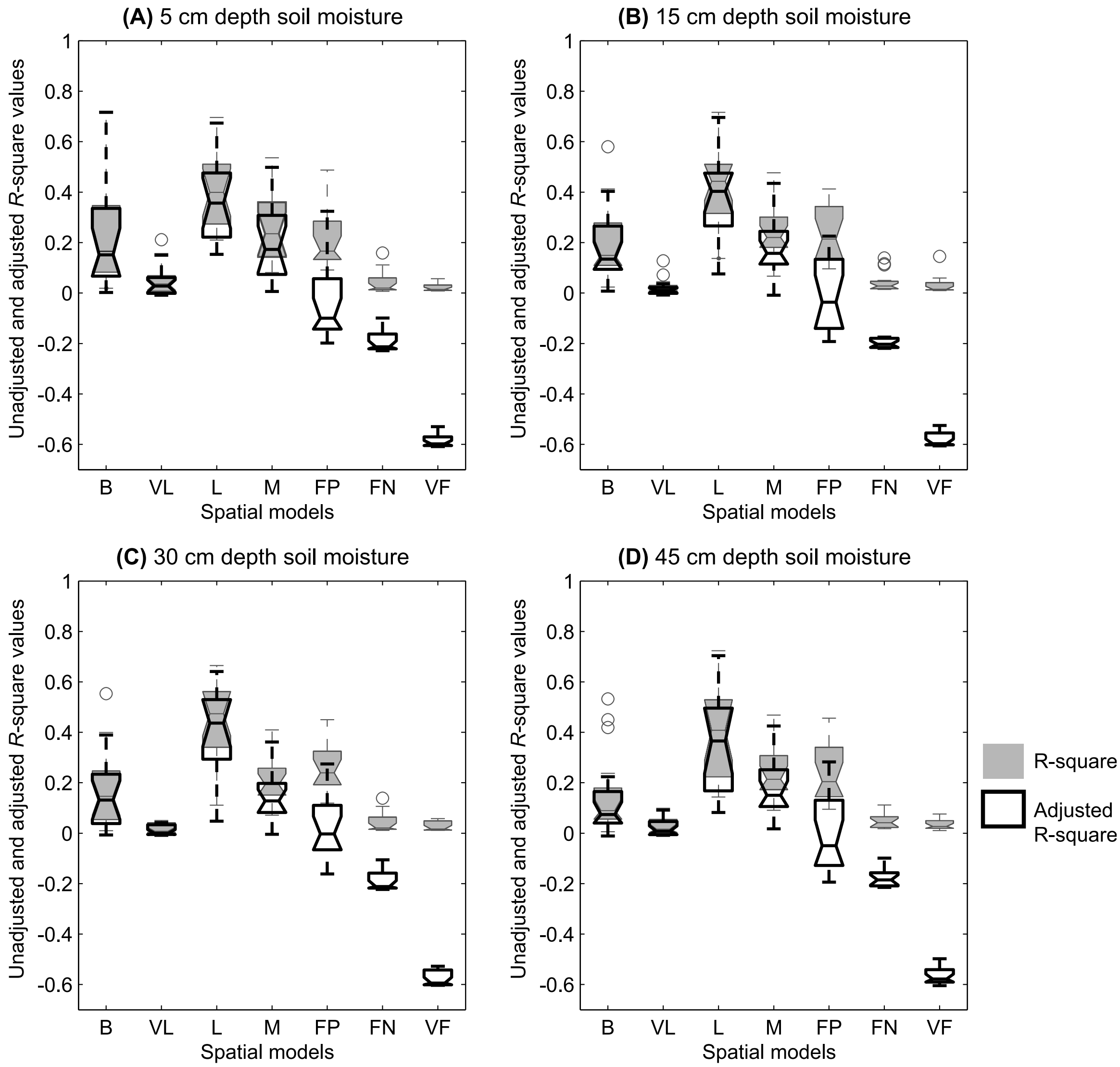

Figure 4. Summary of scale-dependent soil moisture explained variance for the trend and distance-based Moran's eigenvector map submodels. Circles represent statistical outliers. Notches show the 95% confidence interval in the median for box-to-box comparison. B, broad; VL, very large; L, large; M, meso; FP, fine positive; FN, fine negative; VF, very fine.

the analyses are combined to compute the amount of variation explained uniquely by each explanatory table and jointly by two tables. The rather simple algebra is described in *Borcard et al.* [1992] and *Legendre and Legendre* [1998]. In our case, variation partitioning helped discriminate four fractions of variation, namely, the variation in soil moisture at each scale (i.e., B, VL, L, M, FP, FN, or VF) that is (1) uniquely explained by local controls (fraction [a]); (2) uniquely explained by nonlocal controls (fraction [c]), (3) explained by the joint effect of local and nonlocal controls (fraction [b]), and (4) unexplained by any of the topographic variables included in our analysis (fraction [d]). The contribution of each group of topographic variables to the explanation of the soil moisture structure at each scale was quantified using R^2_α and illustrated using Venn diagrams. Individual fractions of variance were tested for significance ($p < 0.05$) using permutation tests. Joint effects could not be tested for significance, because they cannot be obtained directly by a canonical analysis. Following variation partitioning, we kept the "fitted site scores" (hereafter called "fractions fitted site scores") associated with fractions [a + b + c], [a], and [c]. These fractions fitted site scores would be used to map the strength of the spatial control that each topographic variable bears on soil moisture at each scale.

[25] All statistical analyses were done using the spacemakeR package [*Dray et al.*, 2006], the Vegan package (Vegan package data available at http://cc.oulu.fi/~jarioksa/softhelp/vegan.html), and some custom-made functions in the *R* environment [*R Development Core Team*, 2009].

4. Results

4.1. Characteristic Scales of Soil Moisture

[26] Data detrending and DBMEM analysis enabled us to quantify characteristic spatial scales of soil moisture in the Hermine catchment. Preliminary multiple regressions of soil

moisture patterns on the x and y coordinates revealed significant ($p < 0.05$) linear spatial gradients. They correspond to the B-scale structure that explained between 1 and 72% of the soil moisture spatial variation (Figure 4). We assume that this B scale represents the variation occurring at a scale larger than 1.4 ha, since 1.4 ha is the area corresponding to the VL scale (see below). In general, the B-scale soil-moisture-explained variation was the largest at a depth of 5 cm.

[27] For DBMEM analysis, matrix W was created using $d_t = 15$ m. Diagonalization of matrix Ω yielded 116 DBMEM, 58 of which had positive eigenvalues. The progression from large to fine scale was observed with the obtained spatial eigenfunctions: the first DBMEMs illustrate very large scale features, while the last ones characterize very fine scale features (see bubble maps in Figure 3). Regardless of the survey date and measurement depth, the global DBMEM model explained a large proportion of the variation in soil moisture: $0.82 \leq R^2 \leq 0.99$ ($0.21 \leq R^2_\alpha \leq 0.96$). Spatial base functions associated with positive eigenvalues accounted for most of the variation in soil moisture ($0.74 \leq R^2 \leq 0.98$; $0.57 \leq R^2_\alpha \leq 0.96$), whereas base functions associated with negative eigenvalues explained 15% or less of the variation in soil moisture.

[28] DBMEMs were grouped into six spatial submodels based on the size of the patches in the bubble plots (see examples in Figure 3) and on eigenvectors associated with values of the MC significantly different from 0 ($p < 0.05$).

[29] 1. The first spatial submodel was VL (DBMEM 1): $0.85 \leq$ Patches area (ha) ≤ 1.4; MC = 1.05.

[30] 2. The second spatial submodel was L (DBMEMs 2 to 9): $0.54 \leq$ Patches area (ha) ≤ 0.85; $0.83 \leq$ MC ≤ 1.02.

[31] 3. The third spatial submodel was M (DBMEMs 10 to 18): $0.50 \leq$ Patches area (ha) ≤ 0.54; $0.60 \leq$ MC ≤ 0.78.

[32] 4. The fourth spatial submodel was FP (DBMEMs 19 to 47): $0.22 \leq$ Patches area (ha) ≤ 0.50; $0.13 \leq$ MC ≤ 0.58.

[33] 5. The fifth spatial submodel was FN: no DBMEMs were associated with significant values of MC.

[34] 6. The sixth spatial submodel was VF (DBMEMs 71 to 116): $0.02 \leq$ Patches area (ha) ≤ 0.10; $-1.09 \leq$ MC ≤ -0.15.

[35] The global variation in detrended soil moisture was unequally partitioned between the DBMEM-derived characteristic spatial scales, as illustrated in Figure 4. Variation mostly occurred at the L scale ($0.05 \leq R^2_\alpha \leq 0.70$), while the VF scale explained no variation in soil moisture patterns at any date nor any depths. The M, FP, and VL scales explained an intermediate portion of the variation in soil moisture at all depths (M: $-0.01 \leq R^2_\alpha \leq 0.50$; FP: $-0.20 \leq R^2_\alpha \leq 0.32$; VL: $-0.01 \leq R^2_\alpha \leq 0.20$). For all DBMEM-derived spatial models, the average values of explained soil moisture spatial variation hardly varied among sampling depths (Figure 4).

4.2. Scale-Dependent Influence of Topographic Variables on Soil Moisture

[36] Figure 5 illustrates the strength of the scale-dependent relationships between soil moisture patterns and topographic variables. Variation partitioning following the computations of spatial gradients and DBMEMs showed the presence of linear correlations between the structure of soil moisture at different characteristic spatial scales and topography, which also varies at these scales. At the B scale, topography was responsible for the spatial organization of soil moisture in a proportion of 21 to 53%. This was mainly attributable to nonlocal variables ($0.13 \leq R^2_\alpha \leq 0.46$), while local controls explained much smaller proportions of soil moisture spatial variance ($0.01 \leq R^2_\alpha \leq 0.13$). Topography had a lesser influence on the spatial organization of soil moisture at the DBMEM-derived scales. Nonlocal controls generally explained most of the soil moisture spatial structure at the VL and L scales, while topographic controls were the weakest at the M, FP, and VF scales. For all DBMEM-derived scales, a large fraction of the variation in soil moisture ($0.60 \leq R^2_\alpha \leq 0.99$) could not be explained by any of the studied topographic variables, especially at the finest levels.

4.3. Temporal Dependency of Preferential Scales and Topographic Controls

[37] We found that the spatial scales at which soil moisture content are structured, as well as the explanatory potential of topographic controls, vary along gradients of antecedent conditions. Spearman correlation coefficients were computed between trend and DBMEM-related R^2_α values and surrogate variables for antecedent conditions. Some significant correlations were found when variables such as *AP5*, *AP7*, *AP12*, *AP14*, *DSP5mm*, *DSP30mm*, and *PD_Discharge* were used (Table 2; also see Table 1 for variables definitions). The presence of B-scale spatial structure at the 15 cm depth was positively linked to *DSP30mm* ($r_{\mathrm{Spearman}} = 0.61$, $p < 0.05$), which suggests that broadscale patterns at that depth are not observed immediately after a significant storm event. On the contrary, VL-scale soil moisture spatial structure at that same depth was negatively linked to *DSP30mm* ($r_{\mathrm{Spearman}} = -0.76$, $p < 0.05$), which seems to indicate that coherent 1.4 ha wide patterns settle in soon after significant rainfall inputs in the Hermine catchment. Soil moisture explained spatial variance at the L, M, and FP scales was not significantly linked to most of the surrogate variables for antecedent conditions (Table 3).

[38] The most consistent correlations were obtained between VL-scale-related R^2_α values at depths of 5, 30 and 45 cm and discharges monitored at the catchment outlet on each survey date and in the following days ($0.49 \leq r_{\mathrm{Spearman}} \leq 0.79$, $p < 0.05$) (see Figure 6). Some significant correlations were obtained between the magnitude of the topographic influences on soil moisture (i.e., variation partitioning fractions) and *AP14*, *DSP30mm*, and *PD_Discharge* (Table 4). For example, it appeared that the wetter the prior conditions, the larger the effects of nonlocal controls on VL-scale soil moisture at 5 cm (see positive correlations between fraction [c] and *AP14* and *PD_Discharge* in Table 4). At depths of 30 and 45 cm, however, nonlocal controls at the VL scale were important when antecedent conditions were dry (see positive correlations between fraction [c] and *DSP30mm* in Table 4).

[39] The effects of local and nonlocal controls on VL-scale soil moisture were compared between three contrasted surveys (Figure 7). The 5 October 2007 survey took place at the end of a dry spell, while the 12 October 2007 and 15 July 2008 surveys yielded the wettest patterns in our data set (*AP7* > 30 mm). The main difference between the two wet surveys was the number of days elapsed since the last significant storm event (*DSP20mm* value of 1 day versus 3 days). For the driest survey, the proportion of VL-scale

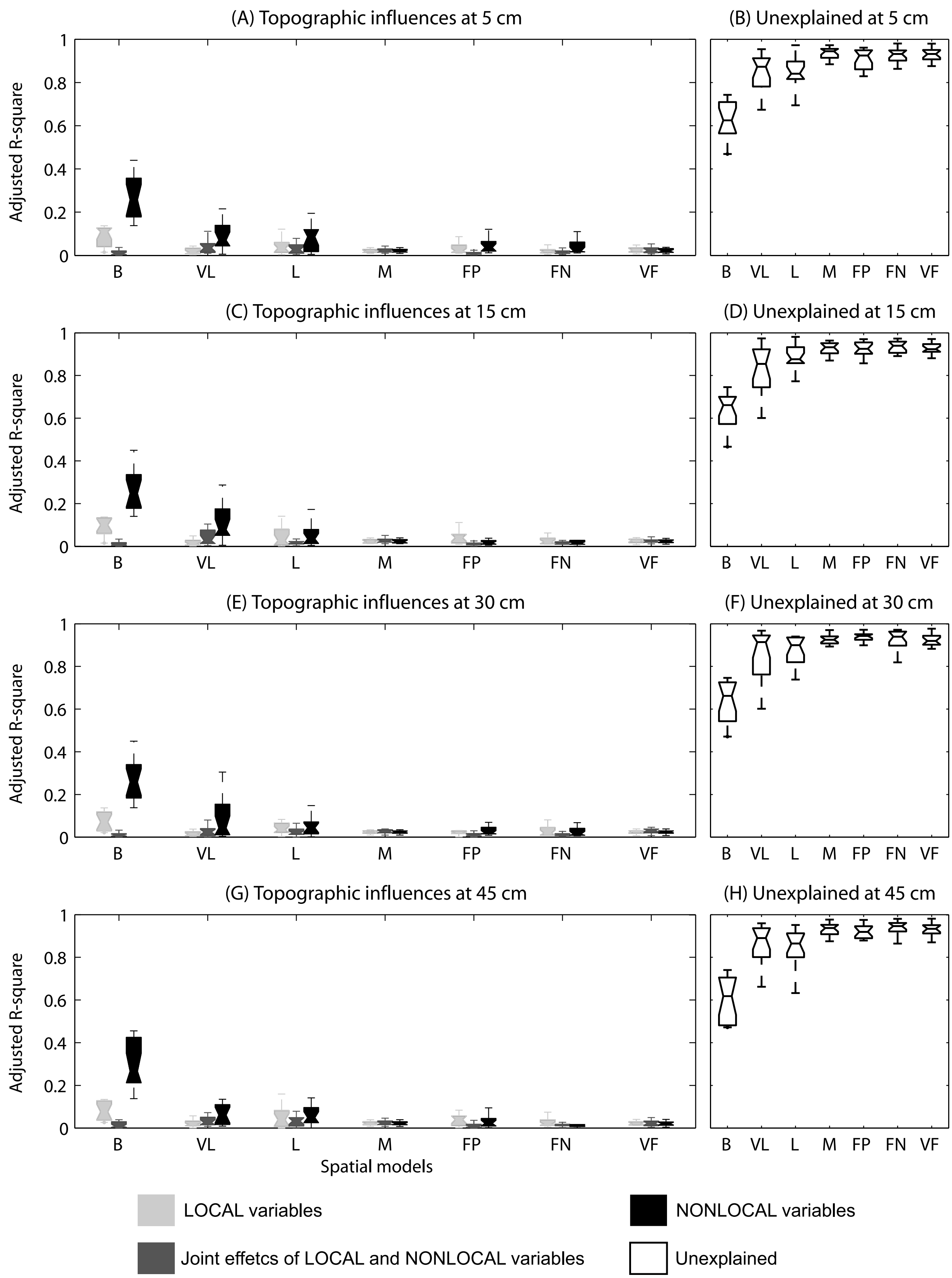

Figure 5. Summary of scale-dependent topographic controls on soil moisture. Notches show the 95% confidence interval in the median for box-to-box comparison. B, broad; VL, very large; L, large; M, meso; FP, fine positive; FN, fine negative; VF, very fine.

Table 3. Spearman Correlation Coefficients Between the Presence of Spatial Structure in Soil Moisture at Each Scale and the Magnitude of Selected Hydrometeorological Variables

Hydrometeorological Variables[a]	cm	Scale[b]						
		B	VL	L	M	FP	FN	VF
PET	5							
	15							
	30							
	45							
AP2	5							
	15							
	30							
	45							
AP5	5			−0.51				
	15							
	30							
	45							
AP7	5							0.52
	15							
	30							
	45							
AP12	5							0.64
	15							
	30							
	45							
AP14	5							0.64
	15							
	30		0.63					
	45		0.65					
DSP5mm	5		0.51					
	15							
	30							
	45							
DSP10mm	5							
	15							
	30							
	45							
DSP20mm	5							
	15							
	30							
	45							
DSP30mm	5							
	15	0.61	−0.76					
	30							
	45					0.54	0.64	0.59
PD_Discharge	5		0.49					
	15							
	30		0.67					
	5		0.61					

[a]See Table 1 for descriptions of hydrometeorological variables.
[b]B, broad; VL, very large; L, large; M, meso; FP, fine positive; FN, fine negative; VF, very fine. Scale is the adjusted R square.

soil moisture spatial variance explained by topography ranged from 14 to 31%, depending on the depth considered. That proportion of explained spatial variance was almost equally distributed between fractions [a], [b], and [c], except at a depth of 30 cm. Similarly, on 12 October 2007, effects of local and nonlocal controls (fractions [a] and [c]) had the same order of magnitude, while joint effects were null. Unlike on 15 July 2008, the influence of nonlocal controls on VL-scale soil moisture was markedly higher than that of local controls. Vegan diagrams shown in Figure 7 hence suggest that the influence of one meteorological variable alone cannot explain the magnitude of topographic influences on soil moisture spatial variation at a given scale. The influence of nonlocal control factors on soil moisture spatial variation at the three largest scales (B, VL, and L) was dependent on not only rainfall amounts (e.g., *AP7*) but also on the way the water inputs were distributed in time (e.g., *DSP20mm*). The VL-scale fraction [a] at all depths was the lowest on 12 October 2007 and 15 July 2008, thus hinting that local controls at that scale are the most significant when prior conditions are dry (e.g., 5 October 2007). Maps of the fractions fitted site scores were drawn to visualize the regions where topographic control on 45 cm soil moisture was the most important at a given scale (Figure 8). Red areas correspond to regions where topographic influences are the most important, whereas blue colored areas correspond to regions where there is a lack of or a weak topographic control. These maps clearly show that topographic influences on the B-scale soil moisture are more important than those on the VL-scale soil moisture (see fraction [a + b + c] maps in Figure 8). For the VL-scale fraction [a] map associated with the 5 October 2007 survey, the sites subjected to the strongest local controls are very few; they correspond to the locations of large boulders and bare outcrops visually identified in the Hermine catchment. The VL-scale nonlocal controls on 15 July 2008 are more "widespread" and located on the moderately steep hill slopes rather than in the bottom valley area (see fraction [c] maps in Figure 8).

5. Discussion

5.1. Scale-Dependent Soil Moisture Variation and Topographic Influences

[40] The global DBMEM model explained a large proportion of the spatial variation in soil moisture at all depths. This is partly attributable to a dense, regular sampling scheme over a fairly small catchment. The explicit quantification of characteristic scales is particularly interesting in the context of a headwater catchment to distinguish the so-called "small scale" and "large scale" over a 5.1 ha region. Values of R^2 and R^2_α (Figure 4) allowed a precise assessment of the hydrological relevance of the scale-dependent critical source areas. Even though we considered a nested spatial framework, it appears that hydrologically relevant processes that produce coherent soil moisture patterns occur at a specific sensitive scale (VL, patches of 0.85 to 1.4 ha) and are not perceptible at the smaller scales (L and M, in particular). This is in accordance with the common assumption in the complex systems theory that the emergent behavior is not the exact sum or the linear extrapolation of its parts. We expected, however, the F and VF DBMEM submodels (less than 0.22 ha) to explain a larger portion of the soil moisture spatial variation given the complex microtopography of the catchment forest floor that may disrupt spatial soil moisture patterns. It is possible that the sampling resolution of 15 m was too coarse to capture such fine-scale variability in soil moisture.

[41] The influence of nonlocal variables on soil moisture was significantly larger at the two largest scales (B and VL) than at the four smallest ones (L, M, FP, and VF). This result is puzzling in the context of a headwater catchment, as it either means that topographic controls should primarily be studied at a scale of 1.4 ha or more or that the two largest scales, especially the B scale, only describe the main hydrological flow gradient across the catchment, i.e., the mainstream channel. The latter hypothesis is the most realistic

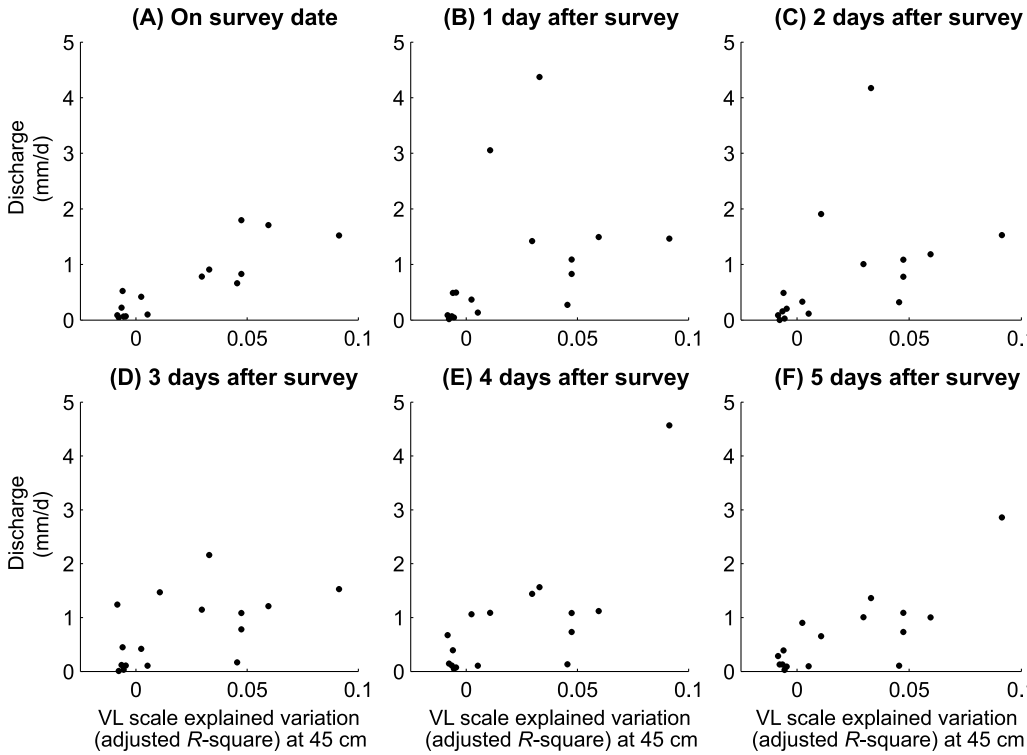

Figure 6. Relationships between the presence of very large (VL)-scale structure (adjusted R-square) in soil moisture at 45 cm and discharge values measured at the catchment outlet ($0.51 \leq R^2 \leq 0.79$).

since the main flow direction, namely, the stream channel in the valley, is the catchment major spatial linear gradient that is not reflected in the detrended soil moisture data used for DBMEM analysis. To avoid such a "bias", one could use undetrended topographic variables to explain the B-scale soil moisture patterns, while detrended topographic variables would be used to explain the detrended moisture patterns at the DBMEM-derived spatial scales. The explanation for local controls having an effect only at the three largest scales may be of a statistical nature rather than hydrological. Several studies have noted that fine-scale patterns identified by DBMEM analysis are often not explained by the available explanatory variables [*Borcard et al.*, 2004; *Bellier et al.*, 2007]. It is also possible that fine-scale features might be influenced by fine-scale topographic variables that are yet to be measured. There was a significant fraction of soil moisture spatial variation at all depths that was not explained by any of the tested topographic variables. Nontopographic yet influential factors like soil texture or hydraulic conductivity could be important variables worth considering in variation partitioning.

5.2. Temporal Dependency of Soil Moisture Structure and Topographic Influences

[42] Given the relatively small soil moisture data set used in this study (16 surveys × 4 depths), it is difficult to build a robust conceptual model of the Hermine catchment behavior across spatial scales and time. However, some of the strongest correlations obtained enable us to say that the B and VL scales were the most responsive to surrogate variables for antecedent conditions. Correlations between next day catchment discharge and VL-scale soil moisture structure (Figure 6) suggest that "critical" source areas should preferably be investigated at the level of 0.85 to 1.4 ha patches. This is plausible, given that source areas are usually well delineated in space and located on the lower hill slopes and in the bottom of the valley at the Hermine. It was also observed that the importance of nonlocal controls for soil moisture spatial variation at the three largest scales (B, VL, and L) was dependent on not only rainfall amounts (e.g., *AP7*) but also on the way the water inputs were distributed in time (e.g., *DSP20mm*, see Figure 7). That observation can be opposed to time-invariant topography-derived upslope contributing areas or wetness indices that are often used in predictive or modeling studies when soil moisture data are missing [*Beven and Kirkby*, 1979; *Barling et al.*, 1994; *Sørensen et al.*, 2006]. Our results indicate that not only real patterns of critical source areas but also the topographic influences they are subjected to are dynamic and highly dependent on antecedent conditions.

5.3. Spatial Filtering Methods and Characteristic Scales: An Improvement or a Burden?

[43] The principal advantage of DBMEM analysis is that it enabled us to partition soil moisture structure over a range of nested characteristic spatial scales and to identify some crucial relations with controlling variables. Conclusions and hypotheses about the Hermine catchment soil moisture dynamics can be drawn for all scales but the finest, especially those modeling negative spatial association. The major drawback of the method is the subjective visual identification of the DBMEM submodels. No other technique but the combination of nested variogram analysis and filter kriging is able to provide such precise estimates of the

Table 4. Spearman Correlation Coefficients Between the Presence of Significant Topographic Controls on Soil Moisture at Each Scale and the Magnitude of Selected Hydrometeorological Variables

Hydrometeorological Variables[a]	cm	Scale[b]						
		B	VL	L	M	FP	FN	VF
				Fraction [a]				
AP14	5							
	15							
	30	0.59						
	45	0.61						0.61
DSP30mm	5							
	15							
	30							
	45						−0.51	
PD_Discharge	5							
	15							
	30							
	45	0.64				0.70		0.85
				Fraction [c]				
AP14	5		0.65					
	15							
	30	−0.65			0.52			
	45	−0.60					0.58	
DSP30mm	5							0.64
	15					0.52		0.74
	30		0.54					0.55
	45		0.49					
PD_Discharge	5		0.74					
	15							
	30	−0.49						
	45	−0.52		0.52			0.53	0.58
				Fraction [d]				
AP14	5							
	15							
	30	0.59						
	45	0.56					−0.63	−0.54
DSP30mm	5							−0.59
	15							
	30							−0.57
	45							
PD_Discharge	5		−0.62					
	15							
	30		−0.49					
	45			−0.61			−0.61	−0.69

[a]See descriptions of hydrometeorological variables in Table 1.
[b]B, broad; VL, very large; L, large; M, meso; FP, fine positive; FN, fine negative; VF, very fine. Scale is adjusted R-square values associated with fractions [a], [c], and [d] in variation partitioning.

spatial variation of a variable across so many different scales as the DBMEM method. *Bellier et al.* [2007] presented an ecological application where they compared PCNM analysis and geostatistical estimation. The combination of nested variograms and filter kriging is not problem free, notably, as far as the identification of fine-scale structure is concerned. *Bellier et al.* [2007] therefore concluded that "for a more objective identification of the relevant scales, both methods need further developments." One of the main differences between geostatistics and DBMEM analysis is philosophical, as one may choose to go for a classical design-based approach (i.e., DBMEM approach) rather than for a probabilistic model-based approach (i.e., geostatistical) [*Bellier et al.*, 2007]. Spatial filtering methods present another advantage for hydrology, as recent developments have led to the use of asymmetric eigenvector maps (AEM) [*Blanchet et al.*, 2008]. AEM are an extension of the MEM framework for directional processes [*Griffith and Peres-Neto*, 2006; *Blanchet et al.*, 2008; *Mahecha and Schmidtlein*, 2008]; they could help us solve the question: At which spatial scale should hydrologic connectivity be defined? Hence, we foresee interesting applications of AEM in hydrological studies where detailed spatial data about drainage networks or subsurface stormflow paths are available.

6. Conclusion

[44] Our objective was to test the effectiveness of a fairly new method to detect characteristic spatial scales in a small temperate humid forested catchment. Through an application to soil moisture data, we have shown that DBMEM analysis is a powerful tool for depicting the spatial structure of hydrological state variables. The global DBMEM model explained 21 to 96% (adjusted R square) of the variation in the detrended soil moisture data apportioned into significant decreasing fractions from the very large scale (0.85–1.4 ha) to the very fine scale (0.02–0.10 ha). The role of catchment topography was also quantified, as the effects

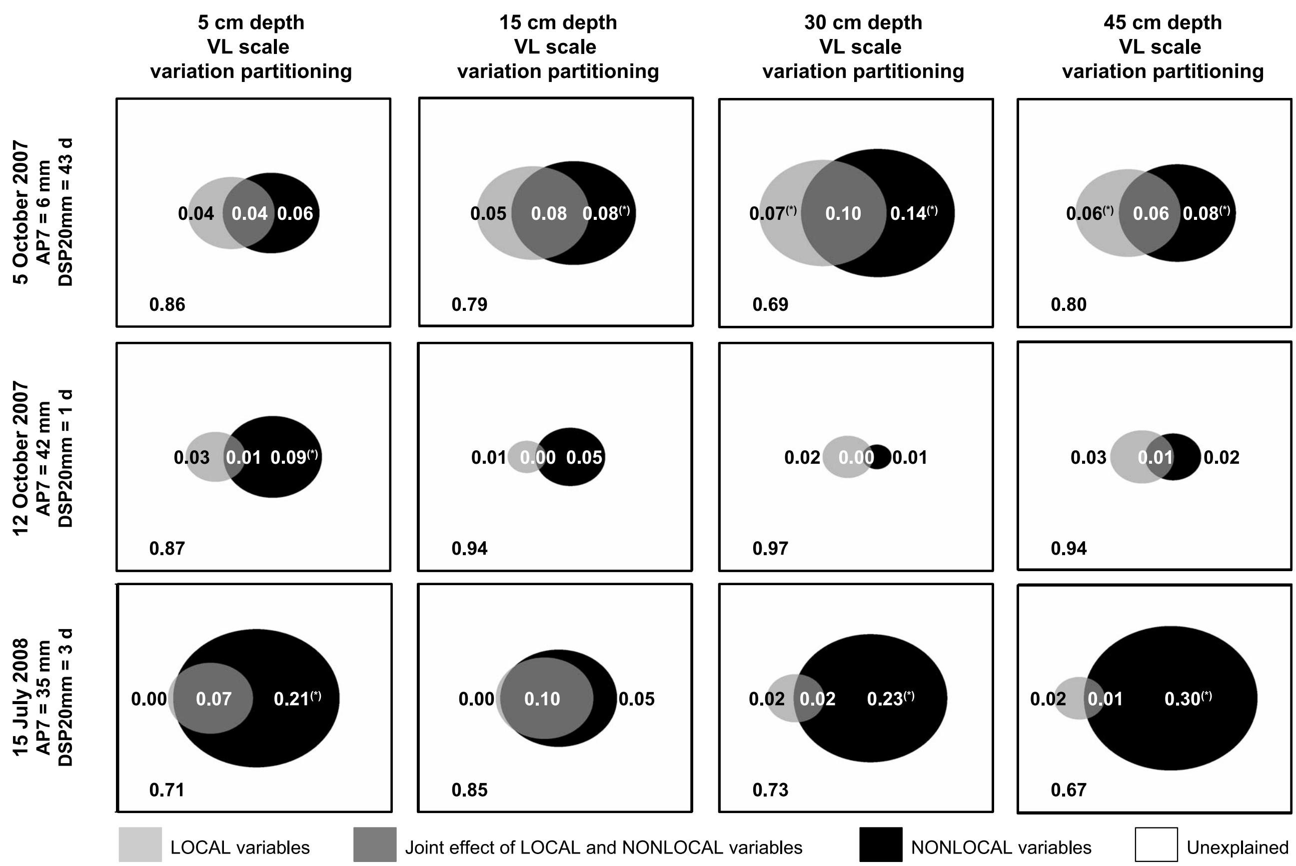

Figure 7. Relative importance of very large (VL)-scale topographic influences on soil moisture for three contrasted surveys. Significant variation partitioning fractions are flagged with an asterisk in parentheses on the Venn diagrams.

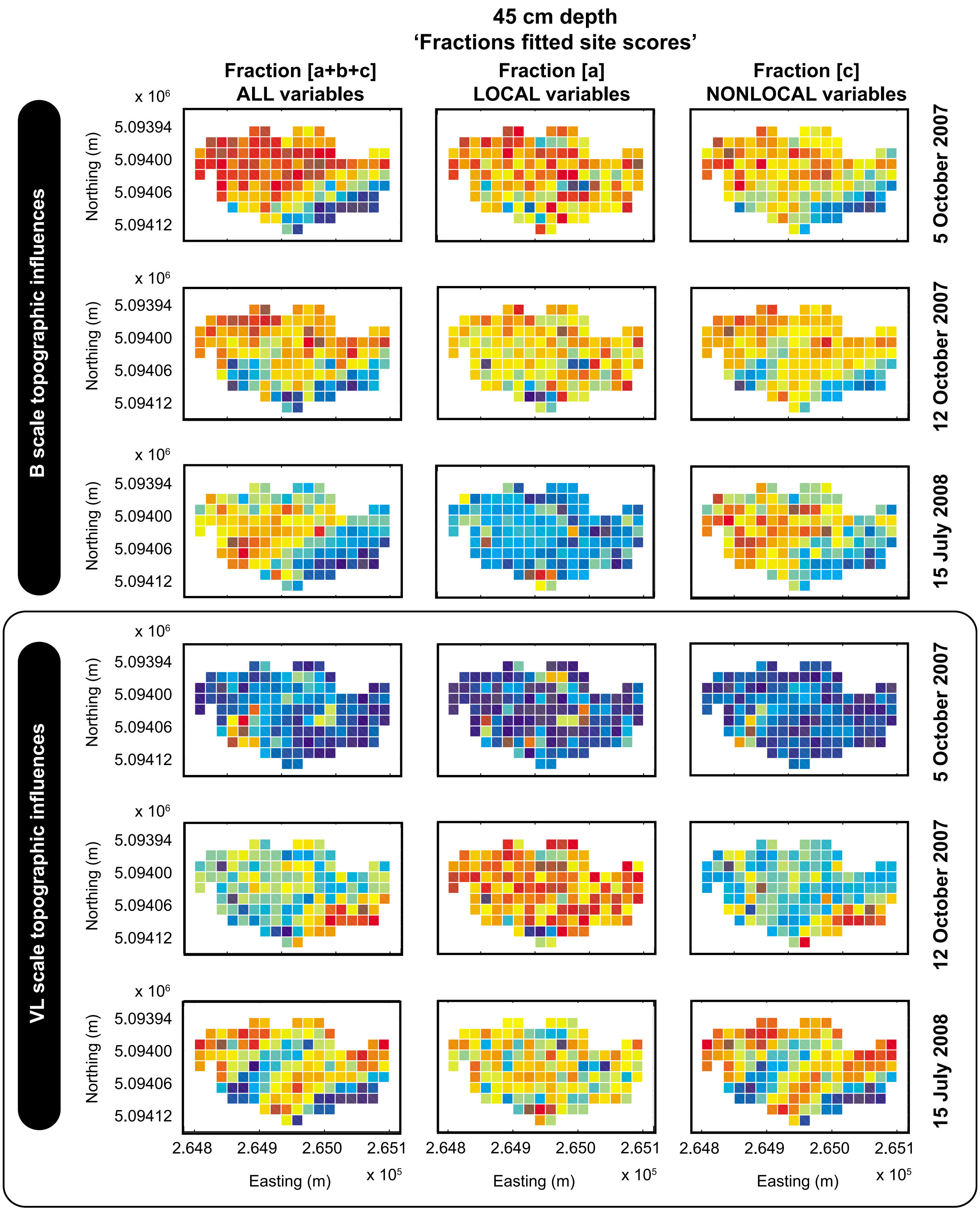

Figure 8. Sample maps of the fitted site scores for three fractions of the variation. Arbitrary units are not shown. Each map/date has its own color scale: orange and red areas show sites that are subjected to the strongest topographic controls on that specific date. B, broad; VL, very large.

of topographic controls, both local and nonlocal, on soil moisture spatial organization were important at the large scale (0.54–0.85 ha) and above. Also, soil moisture broad linear gradients (>1.4 ha) and very large scale spatial patterns were strongly dependent on previous storm properties (antecedent rainfall and days elapsed since the storm). Very large scale soil moisture patterns, in particular, were a good predictor of the catchment hydrologic response. The DBMEM method therefore allowed us to investigate the issue of spatial scale quantitatively rather than qualitatively. Apart from some issues related to spatial structure and effective spatial controls at the fine scale, the combination of DBMEM analysis and variation partitioning was valuable to extract the spatiotemporal relationships between dynamic soil moisture content, static topographic variables, and temporally variable hydrometeorological conditions. The potential of this method should therefore be exploited to test scale-dependent relationships between any hydrologic variable and any environmental variable sampled according to any design in both humid and arid regions. The fact that the DBMEM-derived characteristic spatial scales are nested fits well in the course of recent catchment hydrological studies [e.g., *Cammeraat*, 2002; *Skøien et al.*, 2003; *Soulsby et al.*, 2006; *Didszun and Uhlenbrook*, 2008]. Similarly, future work at the Hermine or in similar environments should involve searching for scale-dependent runoff generation processes that are responsible for scale-dependent soil moisture patterns, topographic controls, and temporal influences on catchment outflows.

[45] **Acknowledgments.** We wish to thank three anonymous reviewers and the associate editor whose comments and suggestions led to a significant improvement of the primary manuscript. We gratefully acknowledge fellowship support of the first author, awarded by the Natural Sciences and Engineering Research Council of Canada and the Fonds Québécois de la Recherche sur la Nature et les Technologies (FQRNT). The research was also funded by the FQRNT. We thank the staff of the Station de Biologie des Laurentides de l'Université de Montréal, Marie-Claude Turmel for her insightful suggestions toward the planning of the soil moisture surveys, and Marius Dulgheru, Gabi Chiaburu, Julie Thérien, Marie Lambois, and Claude Gibeault for their occasional help on the field. We heartily thank our field assistants Rachel Thériault and Katherine Sicotte, who were able to take over the organization of the surveys when needed and contributed great effort in data collection. This study is part of the research program of the Canada Research Chair in fluvial dynamics.

References

Ambroise, B. (2004), Variable, 'active' versus 'contributing' areas or periods: A necessary distinction, *Hydrol. Processes*, *18*(6), 1149–1155.
Barling, R. D., I. D. Moore, and R. B. Grayson (1994), A quasi-dynamic wetness index for characterizing the spatial-distribution of zones of surface saturation and soil-water content, *Water Resour. Res.*, *30*(4), 1029–1044, doi:10.1029/93WR03346.
Bellier, E., P. Monestiez, J. P. Durbec, and J. N. Candau (2007), Identifying spatial relationships at multiple scales: principal coordinates of neighbour matrices (PCNM) and geostatistical approaches, *Ecography*, *30*(3), 385–399.
Beven, K. J., and M. J. Kirkby (1979), A physically based variable contributive area model of basin hydrology, *Hydrol. Sci. Bull.*, *24*, 43–69.
Biron, P. M., A. G. Roy, F. Courchesne, W. H. Hendershot, B. Cote, and J. Fyles (1999), The effects of antecedent conditions on the relationship of hydrology to hydrochemistry in a small forested watershed, *Hydrol. Processes*, *13*(11), 1541–1555.
Blanchet, F. G., P. Legendre, and D. Borcard (2008), Modelling directional spatial processes in ecological data, *Ecol. Modell.*, *215*, 325-336.
Blöschl, G. (2001), Scaling in hydrology, *Hydrol. Processes*, *15*(4), 709–711.
Borcard, D., and P. Legendre (2002), All-scale spatial analysis of ecological data by means of principal coordinates of neighbour matrices, *Ecol. Modell.*, *153*(1–2), 51–68.
Borcard, D., P. Legendre, and P. Drapeau (1992), Partialling out the spatial component of ecological variation, *Ecology*, *73*(3), 1045–1055.
Borcard, D., P. Legendre, C. Avois-Jacquet, and H. Tuomisto (2004), Dissecting the spatial structure of ecological data at multiple scales, *Ecology*, *85*(7), 1826–1832.
Brind'Amour, A., D. Boisclair, P. Legendre, and D. Borcard (2005), Multiscale spatial distribution of a littoral fish community in relation to environmental variables, *Limnol. Oceanogr.*, *50*(2), 465–479.
Cai, X. M., and D. B. Wang (2006), Spatial autocorrelation of topographic index in catchments, *J. Hydrol.*, *328*(3–4), 581–591.
Cammeraat, L. H. (2002), A review of two strongly contrasting geomorphological systems within the context of scale, *Earth Surf. Processes Landforms*, *27*, 1201–1222.
Cassel, D. K., O. Wendroth, and D. R. Nielsen (2000), Assessing spatial variability in an agricultural experiment station field: Opportunities arising from spatial dependency, *Agron. J.*, *92*(4), 706–714.
Didszun, J., and S. Uhlenbrook (2008), Scaling of dominant runoff generation processes: Nested catchments approach using multiple tracers, *Water Resour. Res.*, *44*, W02410, doi:10.1029/2006WR005242.
Dray, S., P. Legendre, and P. R. Peres-Neto (2006), Spatial modelling: A comprehensive framework for principal coordinate analysis of neighbour matrices (PCNM), *Ecol. Modell.*, *196*(3–4), 483–493.
Drouin, D. (1999), Génération d'un modèle numérique d'élévation adéquat pour la modélisation hydrologique d'un petit bassin versant, M.Sc. dissertation, Dept. de Géographie, Univ. de Montréal, Montréal, Quebec, Canada.
Grayson, R. B., A. W. Western, F. H. S. Chiew, and G. Blöschl (1997), Preferred states in spatial soil moisture patterns: local and nonlocal controls, *Water Resour. Res.*, *33*(12), 2897–2908, doi:10.1029/97WR02174.
Green, T. R., and R. H. Erskine (2004), Measurement, scaling, and topographic analyses of spatial crop yield and soil water content, *Hydrol. Processes*, *18*(8), 1447–1465.
Griffith, D. A., and P. R. Peres-Neto (2006), Spatial modeling in ecology: The flexibility of eigenfunction spatial analyses, *Ecology*, *87*(10), 2603–2613.
Hargreaves, G. H. (1975), Moisture availability and crop production, *Trans. ASAE*, *18*, 980–984.
Klemeš, V. (1983), Conceptualization and scale in hydrology, *J. Hydrol.*, *65*, 1–23.
Kumar, P. (1999), A multiple scale state-space model for characterizing subgrid scale variability of near-surface soil moisture, *IEEE Trans. Geosci. Remote Sens.*, *37*(1), 182–197.
Lacey, R. W. J., P. Legendre, and A. G. Roy (2007), Spatial-scale partitioning of in situ turbulent flow data over a pebble cluster in a gravel-bed river, *Water Resour. Res.*, *43*, W03416, doi:10.1029/2006WR005044.
Legendre, P., and L. Legendre (1998), *Numerical Ecology*, 2nd ed., Elsevier Sci., Amsterdam, Netherlands.
Mahecha, M. D., and S. Schmidtlein (2008), Revealing biogeographical patterns by nonlinear ordinations and derived anisotropic spatial filters, *Global Ecolog. Biogeography*, *17*, 284–296.
O'Callaghan, J. F., and D. M. Mark (1984), The extraction of drainage networks from digital elevation data, *Comput. Vision Graphics Image Processing*, *28*, 328–344.
R Development Core Team (2009), R: A language and environment for statistical computing, R Found. for Statistic. Comput., Vienna, Austria. (Available at http://www.R-project.org)
Redding, T. E., G. D. Hope, M. J. Fortin, M. G. Schmidt, and W. G. Bailey (2003), Spatial patterns of soil temperature and moisture across subalpine forest-clearcut edges in the southern interior of British Columbia, *Can. J. Soil Sci.*, *83*(1), 121–130.
Roy, M. L, A. G. Roy, and P. Legendre (2009), The relations between standard fish habitat variables and turbulent flow at multiple scales in morphological units in a gravel-bed river, *River Res. Appl.*, *26*(4), 439–455, doi:10.1002/rra.1281.
Schulz, K., R. Seppelt, E. Zehe, H. J. Vogel, and S. Attinger (2006), Importance of spatial structures in advancing hydrological sciences, *Water Resour. Res.*, *42*, W03S03, doi:10.1029/2005WR004301.
Sibson, R. (1981), A brief description of the natural neighbor interpolant, in *Interpreting Multivariate Data*, edited by D. V. Barnett, John Wiley, Chichester, England, U. K.
Sivapalan, M., and P. C. Young (2005), Downward approach to hydrological model development, in *Encyclopedia of Hydrological Sciences*,

edited by M. G. Anderson, pp. 2081–2100, John Wiley, Chichester, England, U. K.

Skøien, J. O., G. Blöschl, and A. W. Western (2003), Characteristic space scales and timescales in hydrology, *Water Resour. Res.*, *39*(10), 1304, doi:10.1029/2002WR001736.

Sørensen, R., U. Zinko, and J. Seibert (2006), On the calculation of the topographic wetness index: evaluation of different methods based on field observations, *Hydrol. Earth Syst. Sci.*, *10*, 101–112.

Soulsby, C., D. Tetzlaff, S. M. Dunn, and S. Waldron (2006), Scaling up and out in runoff process understanding: insights from nested experimental catchment studies, *Hydrol. Processes*, *20*, 2461–2465.

Tarboton, D. G. (1997), A new method for the determination of flow directions and upslope areas in grid digital elevation models, *Water Resour. Res.*, *33*(2), 309–319, doi:10.1029/96WR03137.

Tromp-Van Meerveld, H. J., and J. J. McDonnell (2006), Threshold relations in subsurface stormflow: 2. The fill and spill hypothesis, *Water Resour. Res.*, *42*(2), W02411, doi:10.1029/2004WR003800.

Weiler, M., J. McDonnell, I. Tromp-van Meerveld, and T. Uchida (2005), Subsurface stormflow, in *Encyclopedia of Hydrological Sciences*, edited by M. G. Anderson, pp. 1719–1732, John Wiley, Chichester, England, U. K.

Western, A. W., R. B. Grayson, G. Blöschl, G. R. Willgoose, and T. A. McMahon (1999), Observed spatial organization of soil moisture and its relation to terrain indices, *Water Resour. Res.*, *35*(3), 797–810, doi:10.1029/1998WR900065.

Western, A. W., R. B. Grayson, and G. Blöschl (2002), Scaling of soil moisture: A hydrologic perspective, *Annu. Rev. Earth Planet. Sci.*, *30*, 149–180.

Western, A. W., S. L. Zhou, R. B. Grayson, T. A. McMahon, G. Blöschl, and D. J. Wilson (2004), Spatial correlation of soil moisture in small catchments and its relationship to dominant spatial hydrological processes, *J. Hydrol.*, *286*(1–4), 113–134.

Woods, R., M. Sivapalan, and M. Duncan (1995), Investigating the representative elementary area concept: An approach based on field data, *Hydrol. Processes*, *9*(3–4), 291–312.

Wu, J., and H. Li (2006), Concepts of scale and scaling, in *Scaling and Uncertainty Analysis in Ecol.: Methods and Applications*, edited by J. Wu, K. B. Jones, H. Li, and O. L. Loucks, pp. 3–15, Springer, Netherlands.

Wu, J., D. E. Jelinski, M. Luck, and P. T. Tueller (2000), Multiscale analysis of landscape heterogeneity: Scale variation and pattern metrics, *Geogr. Inf. Sci.*, *6*(1), 6–19.

G. A. Ali and A. G. Roy, Chaire de Recherche du Canada en Dynamique Fluviale, Département de Géographie, Université de Montréal, C.P. 6128, Montréal, QC H3C 3J7, Canada. (genevieve.ali@umontreal.ca)

P. Legendre, Département de Sciences Biologiques, Université de Montréal, C.P. 6128, Succursale Centre-ville, Montréal, QC H3C 3J7, Canada.